Magnetic Resonance Current Density Imaging of Chemical Processes and Reactions

Katarina Beravs,* Alojz Demšar,† and Franci Demsar*,1

*Institute "Jožef Stefan," Ljubljana, Slovenia; and †Faculty of Chemistry and Chemistry Technology, University of Ljubljana, Ljubljana, Slovenia

Electric current density imaging was used to image conductivity changes that occur as a chemical process or reaction progresses. Feasibility was assessed in two models representing the dissolving of an ionic solid and the formation of an insoluble precipitate. In both models, temporal and spatial changes in ionic concentrations were obtained on current density images. As expected, the images showed significant signal enhancement along the ionization/dissociation sites. © 1999 Academic Press

Key Words: magnetic resonance imaging (MRI); current density imaging (CDI); sodium chloride; calcium carbonate; chemical process.

INTRODUCTION

Electric current density imaging (CDI) is a magnetic resonance imaging (MRI) technique, which enables images of the induced current density and conductivity distributions within a sample of interest. Sensitivity and resolution studies on a model system have shown that similar signal to noise ratios as in conventional MRI can be achieved with CDI (*1, 2*). The technique has already been successfully used on tumors and bones, which shows its potential medical applications (*3–5*). Correlation of current density to ionic concentration has been studied on wood samples (*6*). One of the possible nonmedical applications is the characterization of inorganic chemical processes and reactions (for example ionic reactions, including acid–base neutralizations and reactions that produce precipitates or gases), which change the conductivity by changing the concentration of ions in a solution (*7*).

In this paper, we present the use of CDI as a tool to monitor spatial and temporal changes in ionic concentrations during the dissolving of sodium chloride and the formation of calcium carbonate.

THEORY

CDI is performed by applying bipolar electric currents to the sample by external electrodes. The currents are pulsed synchronously with a standard spin-echo pulse sequence (Fig. 1)

---

[1] To whom correspondence should be addressed. E-mail: franci. demsar@ijs.si.

to produce a quasistatic magnetic field, of which the component parallel to the static magnetic field B_0 is encoded in the image phase (*1, 8*). In contrast to conventional MRI, CDI requires the spatial derivatives of phase images. To image all components of current density, the sample is rotated in the magnet and imaged for three separate orientations in which the x, y, and z axes assigned to the sample are parallel to the B_0 (Fig. 2). Calculating current density j_z in the xy plane requires magnetic field components B_x and B_y.

From the complex nuclear magnetic resonance signal, a phase image in the module of 2π is obtained. First, the B_x field is measured (B_0 is parallel to the x axis of the sample) and second, the B_y field is measured (B_0 is parallel to the y axis of the sample). Between the first and the second step, the sample is rotated in the magnet by 90° about its z axis. Finally, using Ampere's law the current density image is calculated as the difference between a gradient in the x direction of the B_y phase image and a gradient in the y direction of the B_x phase image:

$$ j_z = \frac{1}{\mu_0} \left(\frac{\partial B_y}{\partial x} - \frac{\partial B_x}{\partial y} \right). \qquad [1] $$

EXPERIMENTAL

CDI was tested in two separate experiments: the dissolving of sodium chloride (NaCl), and the formation of calcium carbonate ($CaCO_3$). Both experiments were carried out in plexiglass cells filled with 0.7% agar–agar gel, which was used as a nonconductive medium and to reduce convective motions. A current was passed by two external copper electrodes along the inner walls of the cell and perpendicular with respect to the B_0.

Dissolving Sodium Chloride

The dissolving of sodium chloride in an aqueous medium is a well-known and rapid process. Clustering of water dipoles around the surface of the ionic crystal and the formation of hydrated ions in the solution are the key factors in the dissolving process (*9*). Sodium chloride crystal was shaped as a cylinder (4 mm diameter, length 12 mm) and placed in the
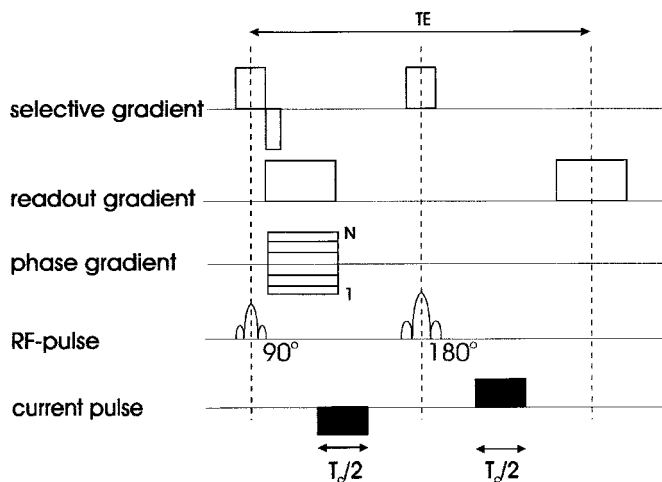
FIG. 1. The current density imaging pulse sequence. The current pulses are of order *mA* and are synchronized with a spin echo pulse sequence as shown.

center of a plexiglass cell. The cell was filled with agar–agar gel, closed with electrodes, and placed in the magnet with its axis perpendicular to the B_0 (Fig. 2). The dissolving process was monitored by CDI in a time course of 0, 5, 10, 15 min, until time τ, when the crystal was dissolved ($\tau = 25$ min).

Formation of Calcium Carbonate

Carbon dioxide gas ($CO_{2(g)}$) is detected by its action on lime water ($Ca(OH)_2$), as a white insoluble precipitate of calcium carbonate ($CaCO_3$) is formed. The $CO_{2(g)}$ can be regenerated by the action of dilute acids on carbonates (*9*). A plexiglass cell (12 mm × 10 mm) containing agar–agar gel doped by a saturated calcium hydroxide ($Ca(OH)_2$) solution was imaged by CDI at time 0. One of the cell walls was then replaced with a Gore Tex membrane and the cell perfused with $CO_{2(g)}$ to form a white insoluble precipitate of $CaCO_3$. Perfusion was done three times. Each perfusion lasted 20 min and was followed by CDI so that the imaging time course was 0, 20, 40 and 60 min. After that, the cell was left in a $CO_{2(g)}$ atmosphere through the night, imaged and then exposed to hydrochloric acid ($HCl_{(g)}$) for 20 min and imaged again. The relevant components of the global stoichiometric equation are (*10*)

$$Ca^{2+} + 2OH^- + CO_2 \rightarrow CaCO_3 + H_2O$$

$$CaCO_3 + 2H^+ + 2Cl^- \rightarrow Ca^{2+} + 2Cl^- + CO_2 + H_2O$$
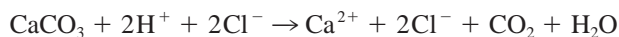
Both experiments were imaged on a 100 MHz Bruker Biospec system equipped with microimaging gradient coils, and a radio-frequency receiver coil (diameter 20 mm), using the pulse sequence shown in Fig. 1. Parameter settings were: repetition time $T_R = 600$ ms, echo time $T_E = 25$ ms, total duration of current pulses $T_c = 10$ ms, field of view FOV =

2 cm, slice thickness 3 mm, number of averages 2, matrix 256 × 256, distance between the electrodes: $l = 12$ mm for the dissolving and $l = 10$ mm for the formation. Voltage applied was $U = 200$ V.

RESULTS AND DISCUSSION

Current density images (Fig. 3) show the onset and progression of the dissolving process. Once the Na^+ and Cl^- ions started to separate from the ionic crystal, the volume area around the crystal became a conductor and thus the flow of the currents produced magnetic fields that were measured by CDI. In line with the progress of the time scale, the concentration of mobile ions in the gel increased. Ions were diffusing away from the crystal until an equilibrium was achieved and the crystal completely dissolved. In the current density images, brighter regions are regions of high mobile ion concentrations and high conductivity (Figs. 3A and 3B). The current density signal is decreasing toward the edges of the cell due to the somewhat slow diffusion of ions (Fig. 3C) into the gel. Figure 3D shows the current density image after 25 min, when the crystal was completely dissolved and the oppositely charged Na^+ and Cl^- ions relatively uniformly distributed in the gel. In the conventional MR images of the sodium crystal dissolution in the gel no distortions, asymmetries, nor susceptibility effects due to the crystal itself, air void, or presence of the electrodes were observed. In the current density experiment, asymmetry is observed, particularly in Fig. 3A. We therefore conclude that this is associated with the inhomogeneity of the system and differences in electrical properties of the constituents.

Calcium hydroxide dissociated in the reaction medium into two oppositely charged ions, Ca^{2+} and OH^-, which made the medium act as a conductor (Fig. 4B). After perfusion with $CO_{2(g)}$, insoluble $CaCO_3$ was produced (solubility product = 4.96×10^{-9}); therefore, the area with $CaCO_3$ had very low current density (*11*). This appears on the current density image as a dark region (Fig. 4D). The reaction with $CO_{2(g)}$ proceeded until all the calcium hydrox-
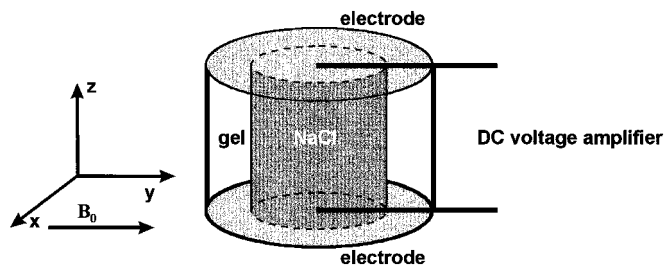

FIG. 2. The plexiglass cell for dissolving NaCl. The cell was designed as a concentric tube, inner diameter 10 mm and height 12 mm, closed at both ends with plate copper electrodes (380 mm²) connected to a DC voltage amplifier. Sodium crystal (length 12 mm and 4 mm diameter) is placed in the center of the cell. Gravity is perpendicular with respect to B_0.
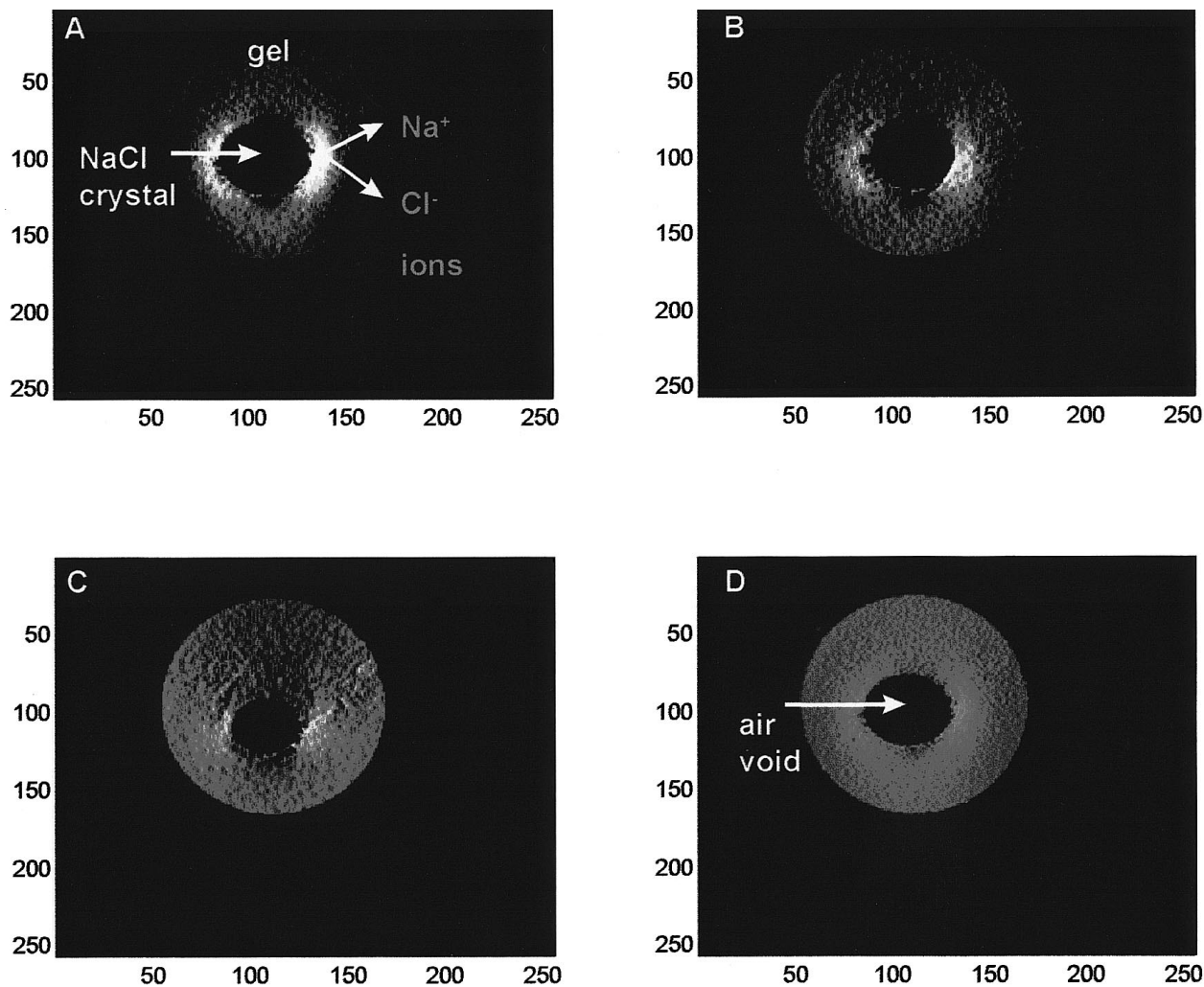
FIG. 3. The dissolving of the NaCl crystal. (A) The current density image was obtained at $t = 0$ of the dissolving process. The white regions show high concentration of Na^+ and Cl^- ions ($j_z = 1500 \pm 25$ A/m^2) around the NaCl crystal. The crystal and the produced ions are labeled with arrows. (B) As the dissolving progressed ($t = 5$ min), more Na^+ and Cl^- ions are present in the gel, making the gel in the cell visible (bright region around the crystal; $j_z = 1450 \pm 30$ A/m^2). (C) The size of the crystal is reduced by half ($t = 15$ min). Almost all the gel in the cell is visible ($j_z = 950 \pm 10$ A/m^2). (D) The crystal is completely dissolved ($t = 25$ min) and the ions are relatively uniformly distributed in the gel, giving a uniform current density signal ($j_z = 1000 \pm 6$ A/m^2). The arrow is pointing to an air void that appeared on the site where the crystal was placed.

ide was transformed into calcium carbonate (Fig. 4F). Calcium carbonate was then dissolved in $HCl_{(g)}$ to calcium chloride ($CaCl_2$). Calcium chloride dissociated into Ca^{2+} and Cl^- ions that regenerated the conductivity of the gel (Fig. 4H). However, calcium hydroxide, calcium carbonate, and calcium chloride in a gel have comparable signal intensities on conventional MR images (Figs. 4A and 4C–4E).

To exclude the influence of stochastic noise, current density images of the gel itself, gel doped with NaCl, and gel doped with $CaCO_3$ without electric current on were obtained and no differences between the images were observed. With the electric current on, the gel itself had no current density, gel doped with NaCl had high current density, and gel doped

with $CaCO_3$ had low current density as shown in both experiments.

CONCLUSIONS

Using the CDI technique it is feasible to monitor spatial and temporal changes in conductivity that occur in a dynamic system such as a chemical process or a chemical reaction. Solid sodium chloride has no magnetic resonance (MR) signal and conventional MR imaging can only show changes in the size of the crystal due to the dissolving. Current density images on the other hand detect the dissolving process as a change in the conductivity of the gel, which
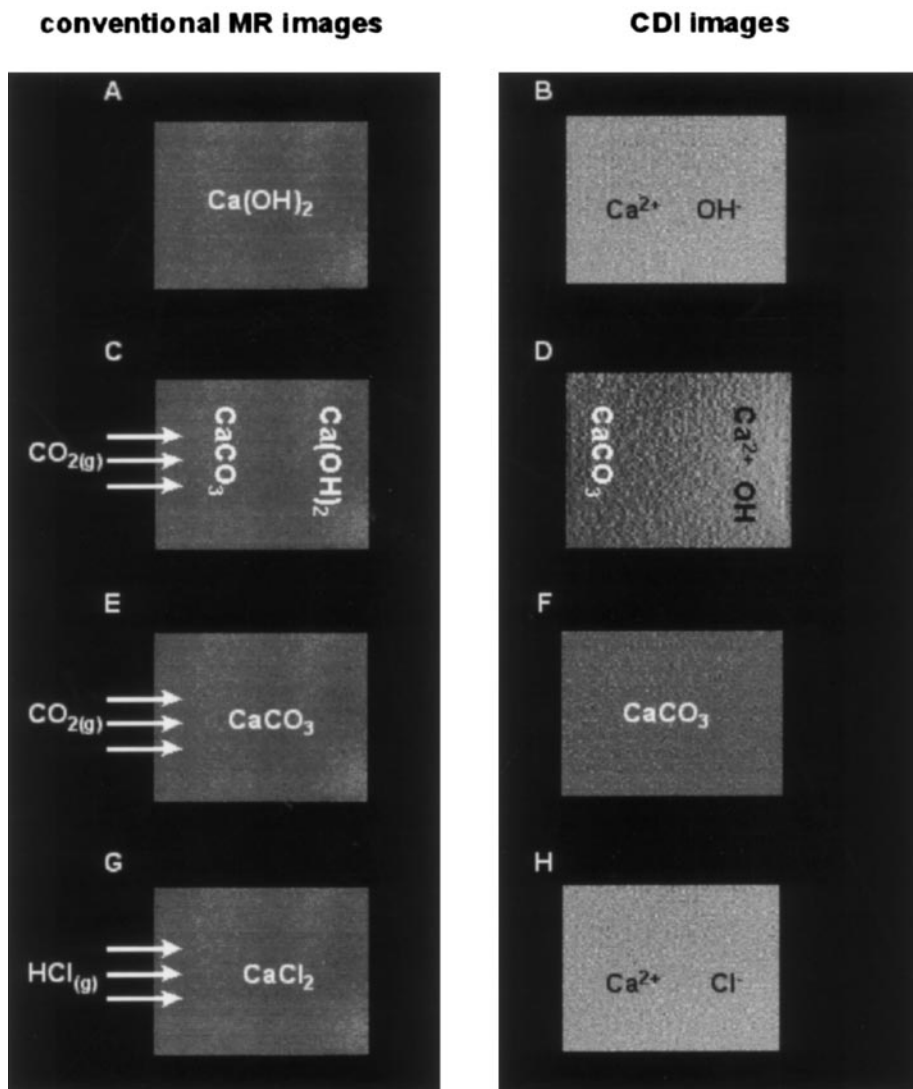
FIG. 4. Conventional MR and current density images of calcium carbonate formation. (A) Agar–agar gel doped by a saturated $Ca(OH)_2$ solution was imaged using conventional MRI. (B) Dissociated $Ca(OH)_2$ produced the current density signal ($j_z = 1100 \pm 10$ A/m^2). (C) One of the cell walls was replaced with a Gore-Tex membrane to allow $CO_{2(g)}$ to diffuse into the gel and react with $Ca(OH)_2$ to $CaCO_3$. There is no difference in the MR signal due to the $CaCO_3$ formation. (D) The current density image shows a line between insoluble $CaCO_3$ (dark region; $j_z = 50 \pm 15$ A/m^2) and dissociated $Ca(OH)_2$ (bright region; $j_z = 1100 \pm 10$ A/m^2) and also clearly marks how far into the gel the reaction has progressed. (E) After 24 h in a $CO_{2(g)}$ atmosphere, all the $Ca(OH)_2$ was converted to $CaCO_3$. (F) The current density image of $CaCO_3$ shows low current density ($j_z = 45 \pm 10$ A/m^2). The cell was afterward perfused with $HCl_{(g)}$ that dissolved $CaCO_3$ to $CaCl_2$. (G) There is no change in the MR signal of $CaCl_2$ compared to $Ca(OH)_2$ and $CaCO_3$ in the images (A), (C), and (E). (H) The current density of the gel is regenerated due to the production of Ca^{2+} and Cl^- ions ($j_z = 1200 \pm 13$ A/m^2).

is a function of the concentration of mobile ions (*6, 8*). Another example is a chemical reaction, where calcium carbonate was produced and dissolved in hydrochloric acid to form calcium chloride. Again, conventional MR imaging does not detect the newly formed substances calcium carbonate and calcium chloride in the reaction mixture since there are enough protons from the reaction medium to produce a uniform MR signal. Current density imaging can differentiate between these two moieties based on their electrical properties. The technique also allows monitoring of the dynamics of the calcium carbonate production; that is,

how far into the gel carbon dioxide diffused to react with calcium hydroxide to calcium carbonate. There are several other chemical reactions that can be monitored by CDI in a way described in this paper. The technique could be of use in studying dissolving processes and reactions of gaseous carbon dioxide, sulphur dioxide and ammonia in water, water solutions, and suspensions. Knowledge of these processes is important in the understanding of carbon, sulphur, and nitrogen cycles in the environment (*12*). Future work will also concentrate on comparison between simulated models and experimental results.

REFERENCES

1. G. C. Scott, M. L. G. Joy, R. L. Armstrong, and R. M. Henkelman, Sensitivity of magnetic resonance current-density imaging, *J. Magn. Reson.* **97,** 235–254 (1992).

2. I. Serša, O. Jarh, and F. Demsar, Magnetic resonance microscopy of electric currents, *J. Magn. Reson. A* **111,** 93–99 (1994).

3. I. Serša, K. Beravs, N. J. F. Dodd, D. Miklavčič, and F. Demsar, Current density imaging of tumours by MRI, *Magn. Reson. Med.* **37,** 404–409 (1997).

4. K. Beravs, D. White, I. Serša, and F. Demsar, Electric current density imaging of bone by MRI, *J. Magn. Reson. Imag.* **15,** 909–915 (1997).

5. D. Miklavčič, K. Beravs, D. Šemrov, M. Čemažar, F. Demsar, and G. Serša, The importance of electric field distribution for effective in vivo electroporation, *Biophysical J.* **74,** 2152–2158 (1998).

6. K. Beravs, P. Oven, N. Torelli, and F. Demsar, Electric current density imaging of oak (*Quercus Rubra L.*) twigs by MRI. *Holzforschung* **52,** 541–545 (1998).

7. J. E. Brady and J. R. Holum, "Chemistry, The Study of Matter and Its Changes," pp. 137–145, Wiley, New York (1996).

8. M. Joy, G. Scott, and M. Henkelman, *In vivo* detection of applied electric currents by magnetic resonance imaging, *Magn. Reson. Imag.* **7,** 89–94 (1989).

9. R. H. Petrucci and W. S. Harwood, "General Chemistry, Principles and Modern Applications," pp. 475–476, Prentice-Hall International, New Jersey (1997).

10. J. D. Lee, "Concise Inorganic Chemistry," pp. 423–424, Chapman & Hall, London (1996).

11. D. R. Lide, "CRC Handbook of Chemistry and Physics," CRC, Boca Raton, FL, (1995).

12. P. O'Neal, "Environmental Chemistry," Chapman & Hall, London (1993).